EVOLUTION OF MILKY-WAY GALAXY: THE SOLAR ELEMENTAL ABUNDANCE CONSTRAINTS.

S. Sahijpal and Tejpreet Kaur, Dept. of Physics, Panjab University, Chandigarh, India 160014 (sandeep@pu.ac.in).

Introduction: The revision in the solar metallicity ($Z_\odot$) from a value of ~0.02 to ~0.014 [1] has significantly influenced the deduced evolutionary history of the solar neighborhood of our galaxy in terms of the evolution of successive generations of stars along with the associated isotopic abundance evolution since the initiation of the formation of the galaxy around ~13 Giga years ago (Gyr.) [2,3]. Here, we present the results of the numerical simulation of the Milky Way galaxy over the galactic distance of 2-18 kpc from the commencement of its origin. The detailed evolutionary history of the accretion of the galaxy, the stellar birth and evolution, and the isotopic abundance evolution of elements up to Zinc is presented. These simulations are not only relevant in understanding the origin of the elemental abundance distribution of stars in our galaxy [e.g., 4,5] but are also relevant to understand the astrophysical context associated with the formation of the solar system [e.g., 6,7].

Numerical Simulations: The classical approach of developing the galactic chemical evolution (GCE) models involves solving the integro-differential equations involving various isotopic species [8,9]. However, several chemodynamical models have been recently proposed that includes the dynamical evolution [10-13]. The approach adopted in the present work is based on the N-body numerical simulations [2,3] that deals with the evolution of successive generations of stars that are synthesized during the accretional growth and evolution of the galaxy. We adopted the traditional two stage in-fall model for the accretion of the galactic halo-thick disk and thin disk [8,9,13]. The galaxy was divided into eight concentric annular rings of width 2 kpc each, starting from 2 kpc from the galactic center to 18 kpc. These rings are numbered {1,2,….8}, and were assumed to have evolved independently in terms of GCE. We have not included radial migration and matter mixing across annular rings. The 4th annular grid defined the solar neighborhood at a distance of 8-10 kpc. The final accreted surface mass density, σ_{Total}, was assumed to vary from 234 to 6 $M_\odot$ pc^{-1} over 2 to 18 kpc [14]. The galactic halo was accreted during the initial 1 Gyr., with a constant surface mass density of 17 $M_\odot$ pc^{-1} from the center to 8 kpc, and a subsequent radial reduction according to r^{-1} in the surface mass density. The star formation rate (SFR) was estimated on the basis of the surface mass density prevailing within an annular ring [2,3,15]. In order to reproduce the observed elemental gradiants, during the galactic evolution subsequent to 1 Gyr., the stellar formation efficiency, 'ν', was assumed to be in the range of 2.3 to 0.24 from the 1st to 8th annular rings, with a value of unity for the 4th ring. These efficiencies were further multiplied by a factor of 2, identically, in all annular rings during the initial 1 Gyr. Depending upon the prevailing SFR, the code stars in the mass range 0.1-100 $M_\odot$ were synthesized according to a piecewise initial mass function (IMF) with three distinct slopes in the power law mass distribution [2]. Successive generations of the code stars were evolved distintly over stellar mass dependent lifetimes. These stars eventually contributed their nucleosynthetic yields [3] to the isotopic inventories of the annular rings. We used the normalized time delay distribution function for the SN Ia rate based on the evolution of binary stars [16]. The simulations were performed with a timestep of one million years (Myr.). The assessments regarding star formation and the mixing of stellar ejecta with interstellar gas were made with an identical time resolution. During the accretion of the galaxy, the infall matter was assumed to have a metallicity identical to the ring at that instant till the ring acquire 0.1 $Z_\odot$. Thereafter, the infall metallicity was assumed to be 0.1 $Z_\odot$.

Results: The predicted SFR, surface mass densities and the various supernovae rates for the various annular rings are presented in Fig. 1, along with the evolutionary trends in the various elemental abundances in Fig. 2. These results correspond to a single set of simulation parameters. The G-dwarf stellar metallicity distribution is also presented in Fig. 1 along with the modulus of the propagation of the cumulative simulation errors (in $M_\odot$) resulting from the various mass balance calculations for the various annular rings. The cumulative error for the entire galaxy is < 0.15 $M_\odot$. The deduced elemental evolutionary treads mostly explains the observational elemental trends of stars.

References: [1] Asplund M. et al. (2009) *ARA&A, 47,* 481-522. [2] Sahijpal S. and Gupta G. (2013) *Meteoritics & Planet. Sci., 48,* 1007-1033. [3] Sahijpal S. (2014) *RA&A,* 14, 693-704. [4] Chiappini C. et al. (2015) *Astrophys. and Space Sci. Procd., 39* (Springer) [5] Anders F. et al. (2017) *A&A, 600,* A70. [6] Huss G. R. and Meyer B. S. (2009), *40th LPSC,* id.1756. [7] Sahijpal S. (2014) *JApA, 35,* 121-141. [8] Chiappini C. et al. (1997) *ApJ, 477,* 765-780. [9] Matteucci F. (2014) The origin of the galaxy and the local group, 145-228 (Springer). [10] Kobayashi C. and Nakasato, N. (2011) *ApJ, 729,* 16-32. [11] Minchev I. et al. (2013) *A&A, 558,* A9. [12] Minchev et al. (2014) *A&A, 572,* A92. [13] Brusadin G. et al. (2013) *A&A, 554,* A135. [14] Rana N.C. (1991) *ARA&A, 29,* 129-162. [15] Alibés A. et al. (2001) *A&A, 370,* 1103-1121. [16] Matteucci F. et al. (2009) *A&A, 501,* 531-538.

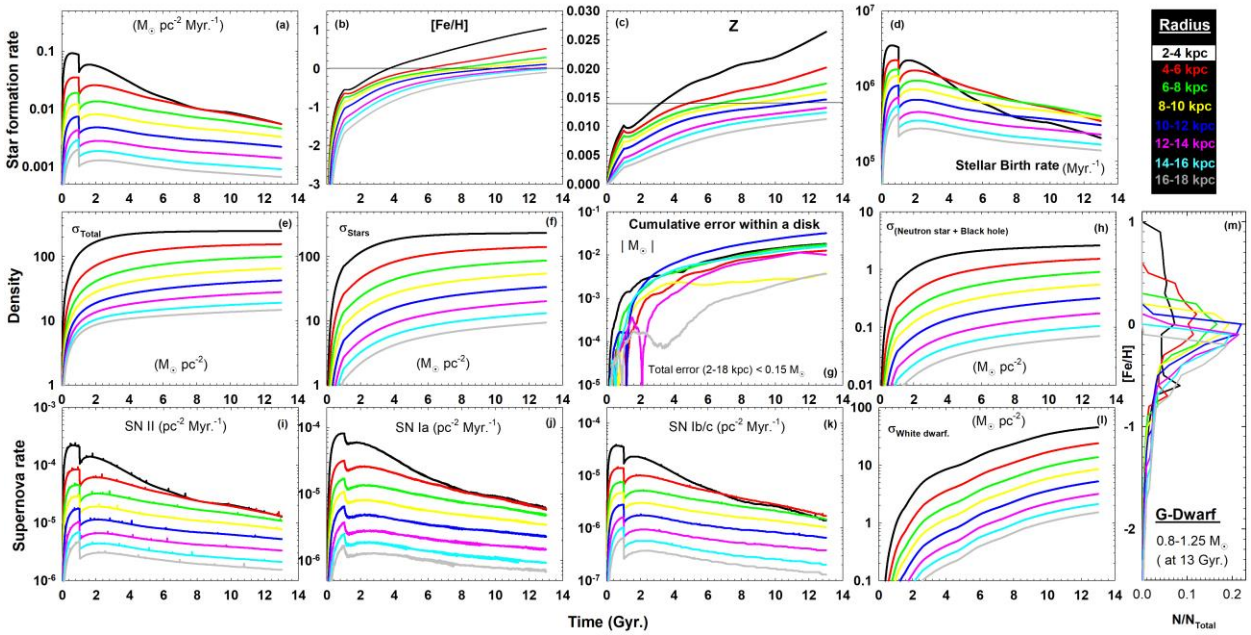

Fig. 1. The numerically deduced, a) star formation rate ($M_\odot$ pc^{-2} $Myr.^{-1}$), b) [Fe/H], c) metallicity Z (*the total mass abundance of all the elements beyond boron*), d) stellar birth rate (in $Myr.^{-1}$), for the various annular rings of 2 kpc width each, starting from 2 to 18 kpc from the galactic center. The deduced, e) total mass density (stars+interstellar gas), σ_{Total} ($M_\odot$ pc^{-1}), f) mass density in terms of the various *live* stars σ_{stars} ($M_\odot$ pc^{-1}) and the mass density of, h) Neutron stars+Black holes and l) white dwarf, are presented for the various annular rings. The deduced supernovae rates for SNII. SNIa and Ib/c are also presented. The stars with mass > 33 $M_\odot$ were considered to evolve through Wolf-Rayet stage followed by SN Ib/c. The birth of the solar system was assumed at 8.5 Giga years (Gyr.), with its present location in the 8-10 kpc annular ring. The deduced, m) stellar distribution of [Fe/H] of the G-Dwarf (0.8-1.25 $M_\odot$) stars at the present epoch (13 Gyr.), and g) propagation of the modulus of the cumulative errors, $|\{(\sigma_{Total} - \sigma_{Gas}) - (\sigma_{stars} + \sigma_{White\ dwarf} + \sigma_{Neutron\ star+Black\ hole})\} \times$ Ring area| (in $M_\odot$) are also presented for the various annular rings. The modulus of the cumulative error for the entire galaxy from 2-18 kpc is < 0.15 $M_\odot$.

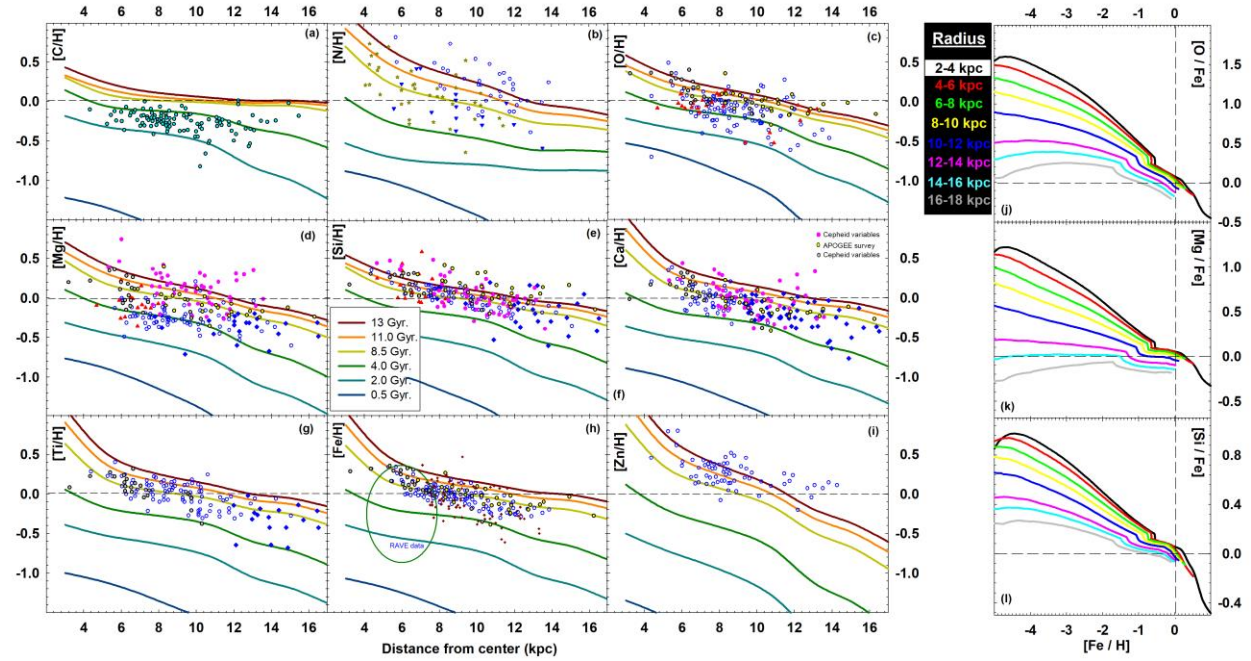

Fig. 2(a-i). Normalized elemental abundance distribution of selective elements across the galaxy at six distinct epochs of evolution. Here, $[A/C] = Log_{10}\{(A/C)_{Ring} / (A/C)_\odot\}$. The observed elemental abundance data of Cepheid variables and Red-giant stars are also presented for reference. **Fig. 2(j-l).** The normalized evolution of [X/Fe] vs. [Fe/H] at various annular rings. The normalization in all cases is done with respect to the solar abundance at 8.5 Gyr. at the solar annular ring between 8-10 kpc.